Arabidopsis RGLG2, Functioning as a RING E3 Ligase, Interacts with AtERF53 and Negatively Regulates the Plant Drought Stress Response[1][W][OA]

Mei-Chun Cheng[2], En-Jung Hsieh[2], Jui-Hung Chen, Hsing-Yu Chen, and Tsan-Piao Lin*

Institute of Plant Biology, National Taiwan University, Taipei 10617, Taiwan

Transcriptional activities of plants play important roles in responses to environmental stresses. ETHYLENE RESPONSE FACTOR53 (AtERF53) is a drought-induced transcription factor that belongs to the AP2/ERF superfamily and has a highly conserved AP2 domain. It can regulate drought-responsive gene expression by binding to the GCC box and/or the dehydration-responsive element in the promoter of downstream genes. Overexpression of *AtERF53* driven by the cauliflower mosaic virus 35S promoter resulted in an unstable drought-tolerant phenotype in T2 transgenic Arabidopsis (*Arabidopsis thaliana*) plants. Using a yeast two-hybrid screen, we identified a RING domain ubiquitin E3 ligase, RGLG2, which interacts with AtERF53 in the nucleus. The copine domain of RGLG2 exhibited the strongest interacting activity. We also demonstrated that RGLG2 could move from the plasma membrane to the nucleus under stress treatment. Using an in vitro ubiquitination assay, RGLG2 and its closest sequelog, RGLG1, were shown to have E3 ligase activity and mediated AtERF53 ubiquitination for proteasome degradation. The *rglg1rglg2* double mutant but not the *rglg2* or *rglg1* single mutant exhibited a drought-tolerant phenotype when compared with wild-type plants. AtERF53-green fluorescent proteins expressed in the *rglg1rglg2* double mutants were stable. The *35S:AtERF53-green fluorescent protein/rglg1rglg2* showed enhanced AtERF53-regulated gene expression and had greater tolerance to drought stress than the *rglg1rglg2* double mutant. In conclusion, RGLG2 negatively regulates the drought stress response by mediating AtERF53 transcriptional activity in Arabidopsis.

In plant stress responses, transcriptional regulatory networks affecting stress-responsive gene expression play central roles in conferring stress tolerance and protecting plants from adverse environmental conditions. High temperatures, drought, and high salinities are common abiotic stresses that adversely affect plant growth and crop production. Plant stress responses are regulated by multiple signaling pathways that activate gene transcription and the downstream machinery. In the signal transduction network from the perception of stress signals to stress-responsive gene expression, various transcription factors (TFs) and cis-acting elements in stress-responsive promoters function in a plant's adaptation to environmental stresses (Shinozaki and Yamaguchi-Shinozaki, 2007).

The AP2/ERF superfamily is defined by the AP2/ERF domain, which consists of about 60 to 70 amino acids and is involved in DNA binding. The ERF family is the largest family that encodes transcriptional regulators and contains 122 genes in Arabidopsis (*Arabidopsis thaliana*; Nakano et al., 2006). The AP2/ERF family is divided into 12 groups based on a phylogenetic analysis of DNA sequences. The ERF domain was shown to specifically bind to a GCC box, which is a DNA sequence involved in the ethylene-responsive transcription of genes (Ohme-Takagi and Shinshi, 1995). It also recognizes the dehydration-responsive element (DRE) in target promoters. The DRE (5′-TACCGACAT-3′) was first identified in the promoter of the drought-responsive *RD29A* gene from Arabidopsis (Yamaguchi-Shinozaki and Shinozaki, 1994). Similar cis-acting elements, named the C-repeat (CRT) and the low-temperature-responsive element, both containing an A/GCCGAC motif that forms the core of the DRE sequence, regulate cold-inducible promoters (Thomashow, 1999). Many genes in groups III (i.e. *DREB1*) and IV (i.e. *DREB2*) were shown to be involved in abiotic stress tolerance.

DREB1 genes are induced by low temperature, whereas *DREB2* homologs are induced by drought and high-salt stress. In spite of the increase in endogenous levels of abscisic acid (ABA) after stress treatments, *DREB2* is not induced by exogenous ABA, suggesting that its function is independent of this hormone (Liu et al., 1998). On the other hand, evidence was provided that both the cold-inducible DREB1 TFs and non-cold-inducible DREB1D may be involved in the activation of the CRT/DRE by ABA treatment (Knight et al., 2004). Previous reports suggested that

[1] This work was supported by the National Science Council, Taiwan (grant nos. 97–2621–B–002–007–MY3) and National Taiwan University (grant nos. 98R0066-35 and 10R80917-1 to T.-P.L.).

[2] These authors contributed equally to the article.

* Corresponding author; e-mail tpl@ntu.edu.tw.

The author responsible for distribution of materials integral to the findings presented in this article in accordance with the policy described in the Instructions for Authors (www.plantphysiol.org) is: Tsan-Piao Lin (tpl@ntu.edu.tw).

[W] The online version of this article contains Web-only data.

[OA] Open Access articles can be viewed online without a subscription.

www.plantphysiol.org/cgi/doi/10.1104/pp.111.189738

overexpression of the constitutively active *DREB2A* resulted in significant drought stress tolerance in transgenic Arabidopsis plants (Sakuma et al., 2006). DREB2A requires posttranslational modification for its activation and was proven to be degraded by the 26S proteasome through DREB2A-Interacting Protein1 (DRIP1)-mediated ubiquitination under nonstressed conditions. DRIP1 is a RING domain E3 ligase isolated from yeast two-hybrid screening, and the *drip1drip2* double mutant exhibits a drought-tolerant phenotype (Qin et al., 2008). Moreover, overexpression of the full-length DREB2A revealed it to be more stable in a *drip1-1* background than in the wild-type one. Qin et al. (2008) also found that overexpression of *DRIP1* delayed the expression of DREB2A-regulated drought-responsive genes. Drought-induced gene expression was also significantly enhanced in *drip1drip2* double mutants under dehydration stress.

Ubiquitination is a common regulatory mechanism in all eukaryotes and selectively targets a diverse range of substrates, including hormone receptors, light regulators, TFs, and damaged proteins for degradation by the 26S proteasome, and affects a range of cellular processes, such as hormone signaling, embryogenesis, photomorphogenesis, circadian rhythms, floral development, senescence, disease resistance, and abiotic stress responses (Vierstra, 2009; Yee and Goring, 2009).

Ubiquitin's attachment to its target protein for modification is conserved in all eukaryotes, and the conjugation cascade involves three consecutive enzymes, E1 (ubiquitin-activating enzyme), E2 (ubiquitin-conjugating enzyme), and E3 (ubiquitin ligase) ligases (Glickman and Ciechanover, 2002). Ubiquitination mediated by E1, E2, and E3 conjugates either single- or multiple-ubiquitin molecules to the target protein, thus enabling the ubiquitin-labeled protein to be recognized by the 26S proteasome and targeted for degradation. Ubiquitin can itself be a substrate for ubiquitination: it is a 76-amino acid protein and has seven Lys residues that can serve as sites of modification (Yin et al., 2007). Ubiquitination of the target protein can end in proteasomal degradation or is associated with nonproteolytic signaling (Pickart and Eddins, 2004; Yin et al., 2007). Linkage of ubiquitin to Lys-48 of another ubiquitin moiety forms the most prominent chain type and targets substrates for recognition and degradation by the proteasome (Yin et al., 2007). In the process, the E3 is the last step in the transfer of ubiquitin but is also responsible for recruiting the target protein for ubiquitination. E3 is considered the major substrate recognition component of the pathway.

The large number and diversity of E3 ligases confer specificity upon the ubiquitination pathway. E3 ligases are subdivided into the HECT, U-box, and RING domain classes (Smalle and Vierstra, 2004) in Arabidopsis. In total, 469 predicted RING and modified RING domain-containing E3 ligases can be grouped into eight subgroups based on the type of RING domain (Stone et al., 2005). The RING domains of ubiquitin ligases serve as docking sites for E2 with thioester-linked ubiquitin and substrate together (Pickart, 2001).

Many cis- and trans-acting elements that function in stress-responsive gene expression were precisely analyzed to elucidate the molecular mechanisms of gene expression in response to drought stress. Herein, we were interested in determining more TFs that are involved in the drought stress signaling pathway. According to the microarray data (Seki et al., 2002), we selected a highly drought-induced gene, *ETHYLENE RESPONSE FACTOR53 (AtERF53* Nakano et al., 2006; *At2g20880*), which was induced by 24.5-fold in the early stage of drought treatment, for this functional study. This putative TF belongs to group I of the AP2/ERF family (Nakano et al., 2006) or the A-6 group of the DREB subfamily (Sakuma et al., 2002). According to the protein microarray data results of AtERF53 (Gong et al., 2008), AtERF53 would bind to both the GCC box and the DRE/CRT element. In this study, we identified a RING domain E3 ubiquitin ligase, RGLG2, that interacts with AtERF53 and mediates its degradation. The *rglg1rglg2* double mutant exhibited a drought-tolerant phenotype. Taken together, we concluded that RGLG2 negatively regulates the drought stress response.

RESULTS

Abiotic Stress Response, Expression Patterns in Different Tissues, and Subcellular Localization of *AtERF53*

Expression patterns of the *AtERF53* gene were analyzed under various abiotic stress conditions and hormone treatments using RNA gel-blot analysis with total RNA isolated from 2-week-old Arabidopsis ecotype Columbia (Col-0) plants grown on Murashige and Skoog (MS) agar medium. The expression of *AtERF53* could not be detected under normal growth conditions. RNA gel-blot results showed that *AtERF53* transcript accumulation was induced within 30 min after exposure to dehydration and salt treatments (Fig. 1A). Under drought and salt treatments, *AtERF53* reached its highest transcript level at the 2-h time point. The increase in *AtERF53* transcript levels occurred before the increase in *COR15B* (a putative downstream gene of *AtERF53*), which was detected 1 h after stress treatment. The RNA gel-blot analysis also showed that the transcript level was not induced within 4 h after application of 100 μM ABA, 100 μM jasmonic acid, or 50 μM 1-aminocyclopropane-1-carboxylate (ACC; Supplemental Fig. S1), whereas the marker gene (*RD29A* for ABA treatment and *EIN2* for ACC and methyl jasmonate treatments) showed specific induced expression.

Histochemical analysis of *GUS* expression in transgenic plants showed that there was no *GUS* expression under normal growth conditions. Seven-day-old seedlings and 2- and 5-week-old T2 transgenic plants were analyzed after 1 h of drought treatment and 30 min of rehydration (Fig. 1B). In 7-d-old seedlings, transgenic

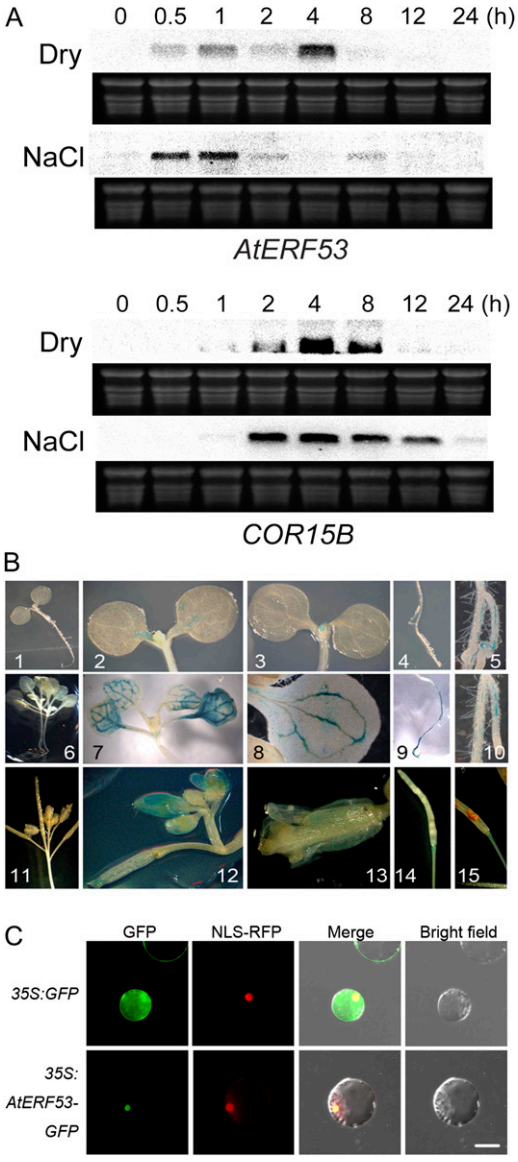

Figure 1. The expression profile of *AtERF53*. A, RNA gel-blot analyses of *AtERF53* and *COR15B* expression by abiotic stresses. Two-week-old seedlings were dried on Whatman 3MM paper (Dry) and treated with 300 mM NaCl (NaCl). B, GUS staining of *AtERF53 promoter:GUS* transgenic plants from different growth stages. GUS activity is shown in transgenic Arabidopsis seedlings grown on MS medium. Panels 1 to 5, One-week-old seedlings; panels 6 to 10, 2-week-old plants; panels 11 to 15, flowers and siliques of 30-d-old plants. Panels 1, 6, and 11 are samples under normal control conditions, and the rest of the samples are with 1 h of drought treatment and 30 min of rehydration. Panels 4, 5, 9, and 10 are root systems. C, Subcellular localization of the AtERF53 protein. *AtERF53* cDNA was fused to GFP, and the construct was expressed in transgenic Arabidopsis under the control of the cauliflower mosaic virus 35S promoter. GFP fluorescence was observed in nuclei of Arabidopsis protoplasts. Bar = 10 μm.

plants showed weak GUS activity in the shoot apical meristem and vascular tissues in leaves and roots. In 2-week-old transgenic plants, GUS activity was observed in leaves and roots, especially in vascular bundles (Fig. 1B). The GUS activity did not occur in guard cells of leaves (data not shown). In 5-week-old transgenic plants, GUS activity was observed in all tissues examined, with low activity in flowers and siliques (Fig. 1B). Expression was detected in sepals of very young closed buds. When the sepals and petals withered, expression was detected at the bottom of the silique, in the abscission zone, and in the pedicel region below that. Strong GUS expression was observed in the vasculature of most tissues.

For subcellular localization of the protein, *AtERF53* cDNA was fused in frame to the C-terminal side of the GFP marker gene, and the resulting construct was introduced into protoplasts isolated from Arabidopsis together with the construct carrying *35S:NLS-RFP* by polyethylene glycol (PEG)-mediated transformation. The *35S:NLS-RFP* construct served as a positive nucleus-targeting control. Green and red fluorescence were detected in nuclei (Fig. 1C).

Overexpressing *AtERF53* Was Unable to Confer Drought Tolerance because of Potential Degradation of the AtERF53 Protein by the 26S Proteasome

Transgenic Arabidopsis constitutively expressing *AtERF53* cDNA (*35S:AtERF53*) was generated. We compared the drought stress tolerance of the *35S:AtERF53* plants with that of wild-type plants. We found that overexpression of *AtERF53* in transgenic plants did not cause improved stress tolerance, suggesting that the AtERF53 protein is unstable or requires posttranslational modification for its activation.

Transgenic Arabidopsis plants harboring an *AtERF53-GFP* construct driven by the 35S promoter were generated in an attempt to determine AtERF53 protein stability in cells. As shown in Figure 2A, the *AtERF53-GFP* transgene was highly expressed in transgenic plants under normal growth conditions, but the GFP fusion protein was not detected in western-blot analysis (Fig. 2B). The AtERF53-GFP protein was not detected in either roots or leaves under normal growth conditions. However, when these plants were treated with the 26S proteasome inhibitor, MG132, clear GFP fluorescence was observed microscopically in both roots and cotyledons (Fig. 2C). GFP fusion proteins were also detected in the western-blot analysis (Fig. 2D). Although the *AtERF53* transgene was expressed under normal growth conditions, the corresponding protein is apparently unstable and may be degraded by the 26S proteasome.

Identification of a RING E3 Ligase Interacting with AtERF53

A yeast two-hybrid screen was performed to identify proteins that interact with AtERF53. Full-length AtERF53 was fused to the yeast GAL4 DNA-binding domain and used as a bait protein for screening against an Arabidopsis cDNA library (under normal

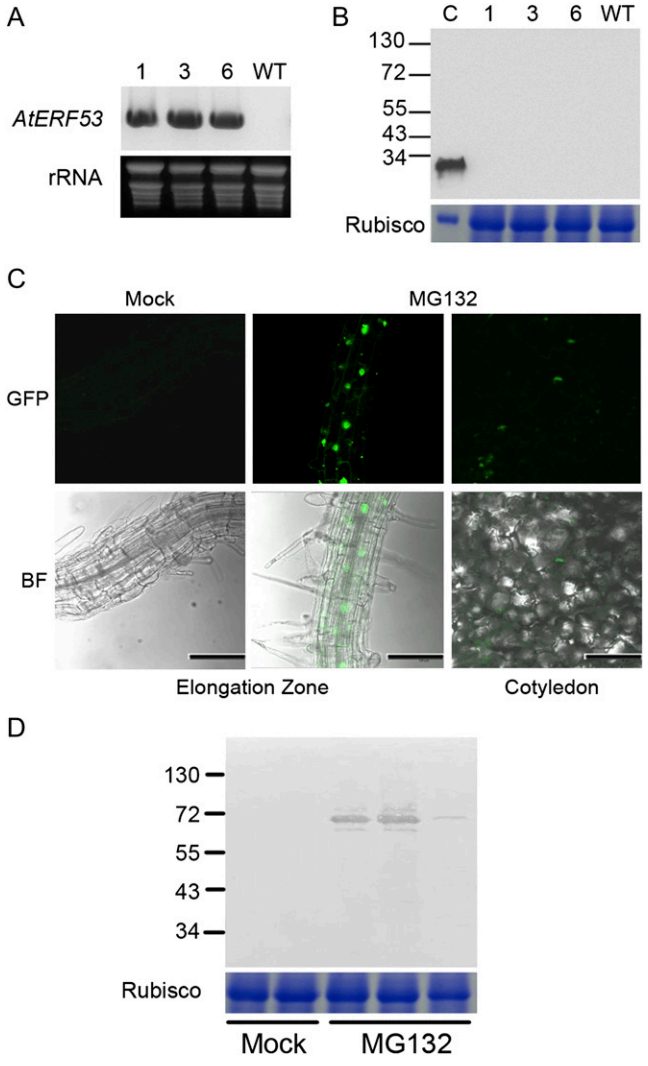

Figure 2. AtERF53 could not be detected in *35S:AtERF53*/Col-0 transgenic plants. A, RNA gel-blot analysis of three overexpressed lines. B, Western-blot analysis of T3 transgenic Arabidopsis plants overproducing *AtERF53*. No AtERF53 protein was detected. Lane C shows the control GFP protein. WT, Wild type. C, Degradation of the AtERF53-GFP protein in the root elongation zone and cotyledons was inhibited by the MG132 proteasome inhibitor. Line 1 of *35S:AtERF53-GFP*/Col-0 was used for MG132 treatment. BF, Bright field. Bars = 50 μm. D, Western-blot analysis of transgenic Arabidopsis plants overproducing AtERF53-GFP under mock and MG132 treatments.

growth conditions) fused to the yeast GAL4 activation domain (AD). Approximately 1.2×10^6 yeast transformants were screened on a synthetic defined (SD) medium lacking Trp, Leu, and His (SD/-T-L-H) plus 1.5 mM 3-amino-1,2,4-triazole. Forty-five positive clones were obtained, and the β-galactosidase activity was individually assessed for all of these clones (Supplemental Table S1). Sequence determination from the clone exhibiting the strongest activity identified a C3HC4 RING domain-containing protein, RGLG2 (for RING domain ligase 2; At5g14420).

Localization of RGLG2-Interacting Domains with AtERF53

According to a previous study (Yin et al., 2007), the RGLG2 structure is shown in Figure 3A. RGLG2 proteins contain a so-called copine (or von Willebrand factor type A) domain. Using protein analysis programs such as pfam, no transmembrane domain was indicated (Yin et al., 2007). Therefore, we designed three different fragments of RGLG2 according to the structure and fused them to the yeast GAL4-AD vector, and each construct was cotransformed into yeast cells with the AtERF53 bait vector. All three kinds of transformed yeast cells could grow well even under several selective conditions (SD/-T-L-H + 20 mM 3-amino-1,2,4-triazole or SD/-T-L-H-A [for adenine]; Fig. 3B). The growth of the yeast cells transformed with negative control vectors was completely inhibited. A β-galactosidase activity assay was performed to verify the interacting activity of the five fragments with the bait mentioned above. The fragment including the copine region of the RGLG2 fragment between amino acids 122 and 424 exhibited the highest β-galactosidase activity (Fig. 3C), supporting this fragment having the strongest interacting activity with AtERF53. And it is sufficient for the protein-protein interaction with AtERF53. This fragment was designed according to the sequence results of yeast two-hybrid screening, suggesting that there might be some posttranscriptional modification of *RGLG2* mRNA or posttranslational modification of the RGLG2 protein.

To determine whether RGLG1, a sequelog of RGLG2, also interacts with AtERF53, full-length RGLG1 was constructed in the yeast GAL4-AD vector and tested in yeast two-hybrid assays. When the construct was transformed into yeast cells containing empty pGBKT7 or the AtERF53 bait construct, all cells could grow on SD/-L-T plates. But on the selective medium, SD/-L-T-H-A, only yeast cells transformed with the constructs RGLG1-AD and AtERF53-BD or T-AD and 53-BD (positive control provided with the Clontech kit) could grow well (Fig. 3D).

RGLG2 Translocalizes into the Nucleus under Salt Stress and Interacts with AtERF53 in Vivo

To further confirm the interaction between RGLG2 and AtERF53 in vivo, we first checked the subcellular localization of RGLG2 in the protoplasts. The protoplasts were transformed with the *35S:RGLG2-GFP* construct by PEG-mediated transformation and observed with fluorescence microscopy. Some GFP signals were observed at the margin of the protoplasts, with lots of accumulated foci in about 43% of transformed protoplasts, and some GFP signals were observed in the nuclei in about 57% of transformed protoplasts (Fig. 4A). To explain this result, we further examined the localization of RGLG2-GFP protein in *35S:RGLG2-GFP* transgenic plants under normal con-

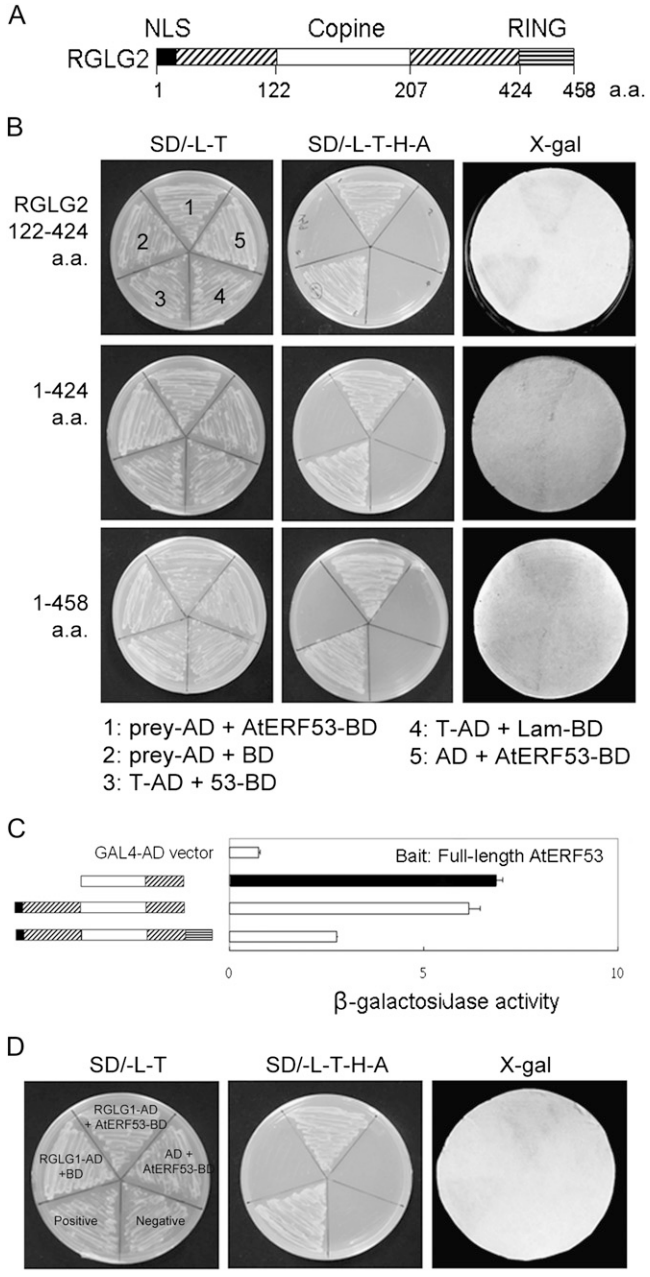

Figure 3. Identification of RGLG interaction with AtERF53 via a yeast two-hybrid analysis. A, Diagram of the specific domains of RGLG2. B, The five yeast clones transformed with the bait, AtERF53, and different lengths of RGLG2 growing on the selective medium and exhibiting β-galactosidase activity. a.a., Amino acids; AD, the pGADT7 vector; BD (for the DNA-binding domain), the pGBKT7 vector; Lam/BD, human lamin C fused to the pGBKT7 vector as a negative control. Every plate has the same labeling as the first labeled plate. C, Localization of the RGLG2 protein interaction domain with AtERF53 using yeast two-hybrid assays. β-Galactosidase activity was measured for each transformant. Error bars indicate SD ($n = 3$). The enzyme activity of the empty vector was defined as 1.0. The diagram for each construct is indicated in the left panel. D, Yeast cells transformed with RGLG1-AD and AtERF53-BD growing on the selective medium and exhibiting β-galactosidase activity.

ditions and under salt stress. As shown in Figure 4B, RGLG2-GFP translocalized from the plasma membrane into the nucleus under salt stress.

In vitro pull-down assays were performed to test the interaction between the full-length RGLG2 protein and AtERF53. RGLG2 was fused to the C terminus of the glutathione *S*-transferase (GST) tag in the pGEX-6p-1 vector and AtERF53 was fused to the thioredoxin (Trx) tag in the pET32a vector. As a result, the full-length Trx-AtERF53 could be pulled down by GST-RGLG2 (Supplemental Fig. S2). A bimolecular fluorescence complementation (BiFC) system was also used to study the interaction between RGLG2/1 and AtERF53 in plant cells (Lee et al., 2008). *RGLG2* was fused to the C-terminal region of the cyan fluorescent protein (CFP), and *AtERF53* cDNA was fused to the N-terminal region of Venus. The two constructs were cotransfected into Arabidopsis protoplasts. The empty vectors in combination with each fusion construct were also cotransfected into Arabidopsis protoplasts as negative controls. After about 16 h of incubation, yellow fluorescent protein (YFP) fluorescence was observed in the nuclei of protoplasts in samples cotransfected with *cCFP-RGLG2* and *nVenus-AtERF53*, whereas samples cotransfected with the empty vector and either *cCFP-RGLG2* or *nVenus-AtERF53* did not yield any YFP signal (Fig. 4C). The BiFC results of RGLG1 interacting with AtERF53 are also shown in Supplemental Figure S3. YFP signals were also observed in the nuclei. These results suggest that both RGLG2 and RGLG1 colocalize and interact with AtERF53 in nuclei of Arabidopsis protoplasts under stress conditions.

RGLG2 Mediates AtERF53 Ubiquitination

We carried out in vitro ubiquitination experiments with the RGLG2 protein to confirm its function as an E3 ligase. Full-length RGLG2 was fused to GST in the pGEX vector. Purified RGLG2-GST fusion protein was mixed with His-tagged ubiquitin, rabbit E1, and human UBCH5c (E2). An immunoblot analysis with anti-ubiquitin showed that ubiquitinated proteins were detected in the presence of all these components (Fig. 5A). Furthermore, an immunoblot analysis with anti-GST showed that RGLG2-GST in the presence of ubiquitin, E1, and E2 was attached to one ubiquitin monomer. As a result, one additional higher molecular weight protein band appeared (Fig. 5B). These results suggest that the RGLG2 protein can be autoubiquitinated in the presence of the E1 and E2 enzymes. As for RGLG1, the ubiquitination assay was also performed to demonstrate its E3 ligase activity using ubiquitin antibody (Supplemental Fig. S3).

In order to determine whether RGLG2 and RGLG1 can mediate AtERF53 protein ubiquitination, we also conducted an in vitro ubiquitination assay using AtERF53 protein as a substrate. Full-length AtERF53 was fused to Trx and a His tag in the pET32a vector, and the recombinant fusion protein was purified by

the His tag affinity to a nickel-nitrilotriacetic acid agarose matrix. An immunoblot analysis with anti-Trx showed that a higher molecular weight shifted band was observed in the presence of ubiquitin, E1,

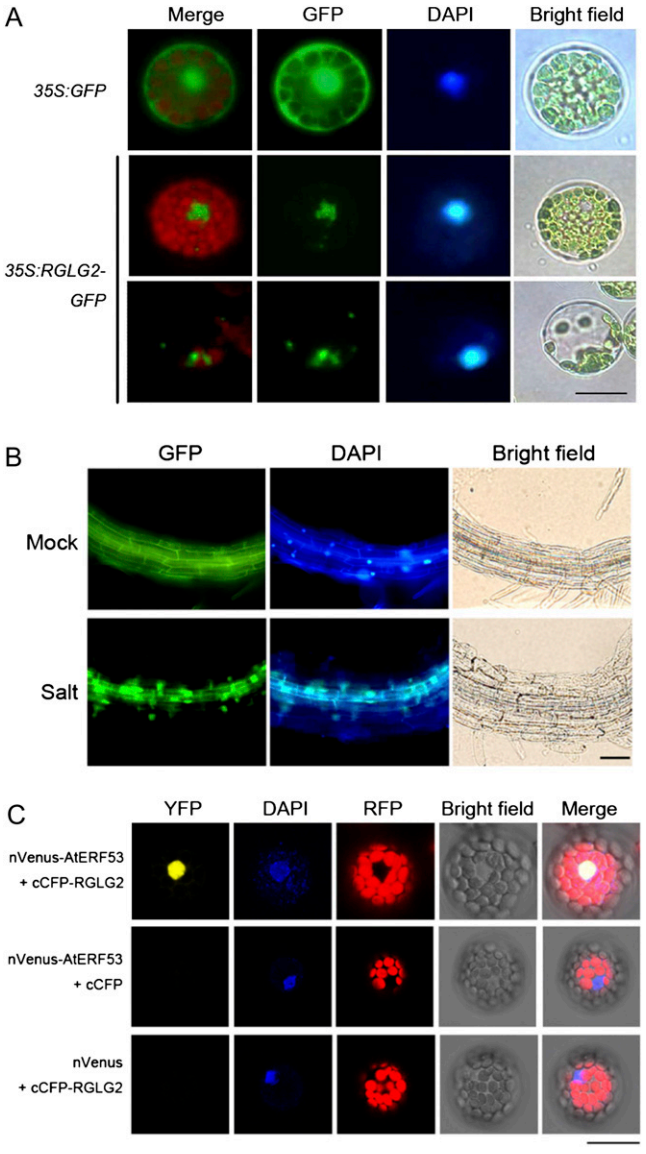

Figure 4. RGLG2 translocalizes into the nucleus under stress conditions and interacts with AtERF53 using the BiFC system. A, Full-length *RGLG2* was fused with *GFP* driven by the cauliflower mosaic virus 35S promoter. Some GFP fluorescence signals were observed in the nuclei and some at the plasma membranes. The experiment was repeated three times, and at least 60 protoplasts were observed. Bar = 10 μm. B, The RGLG2-GFP observed in *35S:RGLG2-GFP* transgenic plants translocalized from the plasma membrane into the nucleus under salt stress. The images were taken after the transgenic plants were soaked in salt solution (200 mM) for 1 h. Bar = 10 μm. C, Interaction between AtERF53 and RGLG2 by BiFC. The top panels show constructs of *cCFP-RGLG2* and *nVenus-AtERF53*. YFP and RFP fluorescence, 4′,6-diaminophenylindole (DAPI; for nuclear staining), bright-field, and merged images are shown for each kind of transformation combination. Bar = 25 μm.

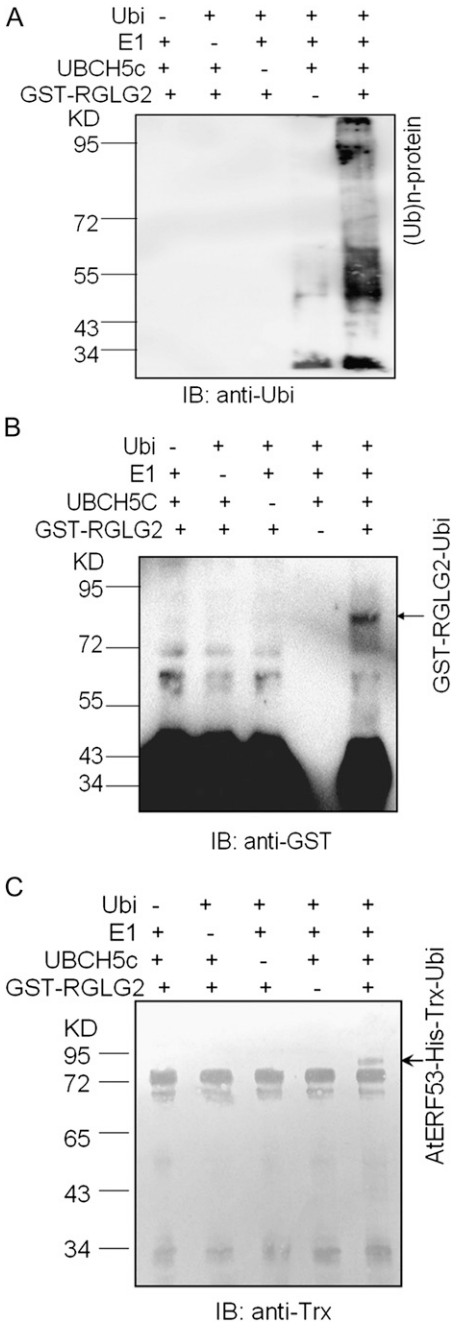

Figure 5. RGLG2 functions as an E3 ubiquitin ligase and mediates AtERF53 protein ubiquitination. A, In the presence of the ubiquitin, E1, and E2 enzymes (UBCH5c), RGLG2-GST fusion proteins displayed ubiquitin E3 ligase activity. Protein bands with ubiquitin attached were detected by an anti-ubiquitin immunoblot (IB) analysis (10% SDS-PAGE). B, Detection of RGLG2-GST autoubiquitination. RGLG2-GST fusion proteins were detected with a GST antibody, and shifted bands indicate the attachment of one or two ubiquitin molecules (10% SDS-PAGE). C, RGLG2 mediates the ubiquitination of the AtERF53 protein. The full-length AtERF53 protein was fused with His and Trx tags (His-AtERF53-Trx) and used as a substrate for the assay. Anti-Trx was used in the immunoblot analysis to detect the Trx-tagged substrate protein (10% SDS-PAGE).

E2, and RGLG2 (Fig. 5C) or ubiquitin, E1, E2, and RGLG1 (Supplemental Fig. S3). The shifted band should correspond to one additional ubiquitin monomer attached to the substrate according to the M_r.

The Double Mutant *rglg1rglg2* Exhibits a Dehydration-Tolerant Phenotype

RGLG2 mRNAs are rather abundant and ubiquitously expressed but with tissue-specific variations (Kraft et al., 2005). According to the microarray data of the online Arabidopsis eFP browser (http://bbc.botany.utoronto.ca/efp/cgi-bin/efpWeb.cgi), Supplemental Figure S4 shows the expression changes of *RGLG2* and *RGLG1* during drought and salt stress treatments. During earlier drought stress treatment, both genes were slightly down-regulated. This might favor the transient accumulation of TF AtERF53 and thus enable plants to acquire a sufficient amount of effective AtERF53 to activate downstream gene expression.

RGLG2's closest sequelog, RGLG1, was not found by our yeast two-hybrid screening. Their functions are redundant according to Yin et al. (2007). We hypothesized that RGLG1 also participates in the interaction with AtERF53. The homozygous *rglg1rglg2* double mutant showed a bush-like phenotype, completely lacking apical dominance. It also showed significant plant growth retardation and a late-flowering phenotype compared with those of the Col-0 wild type and the two single mutants (Fig. 6A). To test the drought stress tolerance of *rglg1rglg2*, water was withheld from 2-week-old double mutant and wild-type plants for about 14 to 16 d, and then they were rewatered for 3 to 5 d. The survival rate of the *rglg1rglg2* double mutant was 58%, which was significantly higher than that of wild-type plants (2%; Fig. 6B). No significant difference was observed between wild-type plants and single mutants (*rglg1* single mutant data not shown).

Overexpression of *AtERF53* in the *rglg1rglg2* Double Mutant Results in Stable AtERF53-GFP Protein Accumulation and Enhanced Drought Tolerance

To confirm RGLG2's and RGLG1's functions in the stability of the AtERF53 protein, we transformed a *35S:AtERF53-GFP* construct into the *rglg1rglg2* double mutant and obtained two independent transgenic lines. Real-time reverse transcription-PCR revealed that the transgene expression in both double mutant and wild-type backgrounds was relatively high, whereas *AtERF53* was expressed at very low levels under normal nonstressed conditions in wild-type plants (Fig. 7A). Interestingly, green fluorescent signals were observed in nuclei of *35S:AtERF53-GFP/rglg1rglg2* but not *35S:AtERF53-GFP/*Col-0 plants (Fig. 7C). We performed an immunoblot analysis to detect the GFP or GFP fusion protein in transgenic plants using anti-GFP. A protein band of approximately 67.5 kD, which is the predicted AtERF53-GFP molecular mass, was detected in two independent *35S:AtERF53-GFP/rglg1rglg2* transgenic lines (Fig. 7B). However, no GFP fusion protein was detected in two *35S:AtERF53-GFP/*Col-0 transgenic lines.

To examine the potential AtERF53-regulated genes, the expression of several drought-responsive genes, such as *RD29A*, *RD29B*, *COR15A*, *COR15B*, and *P5CS1* (for Δ^1-pyrroline-5-carboxylate synthase 1; Pro synthesis correlated), was tested using real-time PCR in transgenic plants. The expression of *COR15B* and *P5CS1* was compared in two different lines from *35S:AtERF53-GFP/rglg1rglg2*, *35S:AtERF53-GFP/*Col-0, and *35S:RGLG2/rglg1rglg2*, and the expression was greater in *35S:AtERF53-GFP/rglg1rglg2* than in *35S:AtERF53-GFP/*Col-0 and the *RGLG2* overexpressor even under nonstressed conditions (Fig. 7D). Drought tolerance tests of *rglg1rglg2* double mutants and *35S:AtERF53-GFP/rglg1rglg2* transgenic plants were also performed. After withholding water for about 21 d, *35S:AtERF53-GFP/rglg1rglg2* transgenic plants showed much greater drought tolerance (67%) than *rglg1rglg2* double mutants (21%; Fig. 7E). We also compared the drought

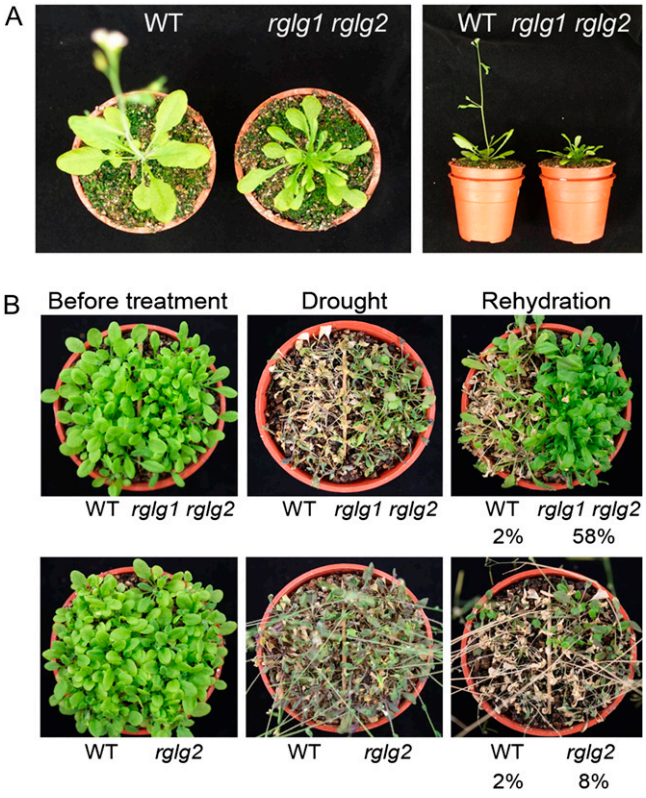

Figure 6. Phenotypic and stress tolerance studies of *rglg1rglg2* double mutants. A, Phenotypes of 3-week-old wild-type plants (WT) and *rglg1rglg2* double mutants. B, Survival rates of wild-type, *rglg2* single mutant, and *rglg1rglg2* double mutant plants after withholding water for 14 to 16 d (Drought) and rehydration for 4 d (Rehydration). Twenty plants (five plants per pot) were tested in each experiment. The survival rate is indicated below the rehydration panels. This experiment was repeated three times with similar results.

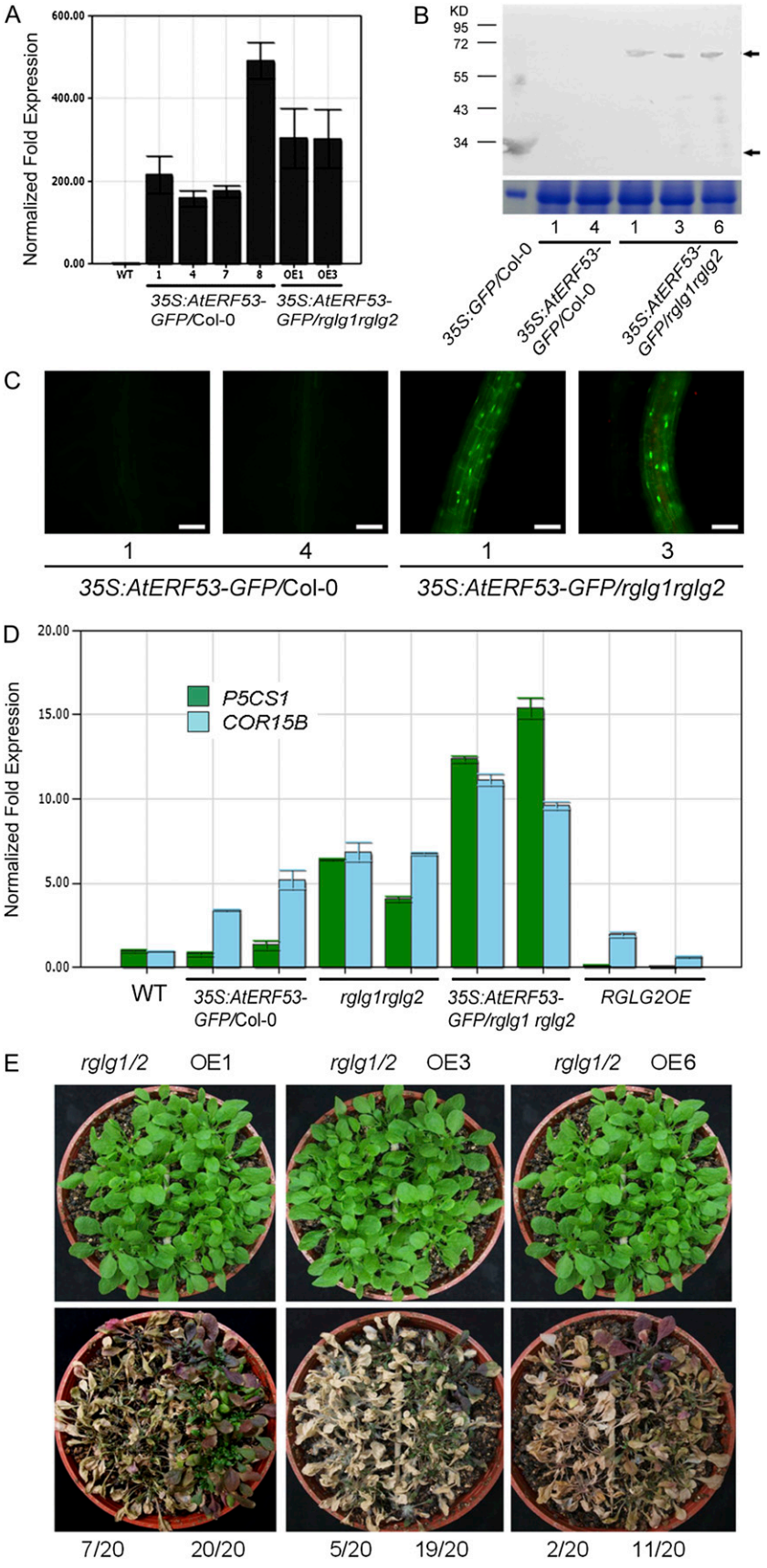

Figure 7. Gene expression and protein detection in *35S:AtERF53-GFP/rglg1rglg2* transgenic plants. A, Relative transgene expression of *AtERF53-GFP* in *35S:AtERF53-GFP/*Col-0, *35S:AtERF53-GFP/rglg1rglg2*, and wild-type plants as measured by real-time PCR. Error bars indicate SD ($n = 3$). B, Protein gel-blot analysis of GFP or AtERF53-GFP protein levels in *35S:GFP/*Col-0, *35S:AtERF53-GFP/*Col-0, and *35S:AtERF53/rglg1rglg2* using the GFP antibody. The bottom arrow indicates the GFP protein band, and the top arrow indicates the AtERF53-GFP fusion protein band. C, Confocal microscopic observation of GFP fluorescence in roots of *35S:AtERF53/rglg1rglg2* (two independent lines) and *35S:AtERF53-GFP/*Col-0 (two lines). Bars = 50 μm. D, Relative gene expression of *COR15B* and *P5CS1* in *35S:AtERF53-GFP/*Col-0, *rglg1rglg2*, *35S:AtERF53-GFP/rglg1rglg2*, *35S:RGLG2/rglg1rglg2* (*RGLG2OE*), and wild-type (WT) plants as measured by real-time PCR. Error bars indicate SD ($n = 3$). E, Drought tolerance test of *rglg1rglg2* double mutants (*rglg1/2*) and *35S:AtERF53-GFP/rglg1rglg2* (OE lines). Numbers under the panels indicate the survival over total plants. This experiment was repeated three times with similar results.

tolerance between the wild type, *rglg1rglg2* double mutants, and the *RGLG2* overexpressor, which is supposed to be like *aterf53* knockout mutants. After withholding water for about 14 d, both the wild type and the *RGLG2* overexpressor showed a non-drought-tolerant phenotype (Supplemental Fig. S5), while *rglg1rglg2* double mutants showed greater drought tolerance than the *RGLG2* overexpressor. We have also examined the Pro contents in the wild type, double mutants, and *35S:AtERF53-GFP/rglg1rglg*. As shown in Supplemental Figure S6, we observed higher Pro levels in both double mutants and overexpression lines than in the wild-type plants. Moreover, overexpression lines contained more Pro than double mutants.

In conclusion, AtERF53 overexpression increases drought tolerance by elevating stress-responsive genes, such as *COR15B* and *P5CS1*, and RGLG1/2 negatively regulates drought stress tolerance by mediating AtERF53 ubiquitination. The stable AtERF53-GFP protein accumulation and drought tolerance experiments provide indirect evidence that RGLG1 plays a redundant role of RGLG2 in regulating the function of AtERF53.

DISCUSSION

In this study, we showed that *AtERF53* was clearly induced at the transcription level by drought, salt, and osmotic stress, but not by ABA, jasmonic acid, or ACC. According to Gong et al. (2008), the AtERF53 protein binds to both the GCC box and DRE probes, using a microarray protein-DNA interaction analysis. This may occur because the GCC box and the DRE motif share a similar core sequence, CCGNC (Gong et al., 2008). AtERF53 joins several TF genes, for example, *DREB2A* (Sakuma et al., 2006), *CBF4* (Haake et al., 2002), and *RAP2.4* (Lin et al., 2008), in the ERF TF family, and many others in different TF families, that work in concert to form a network to help plants in water-deficit environments. A large number of TFs with both positive and negative functions are provoked by dehydration (Seki et al., 2002). Although some are immediate and some are later responses, all of them are down-regulated when the drought signal vanishes. Posttranslational modification by the proteolysis of TFs probably has a major role in keeping TF low or negligible in an unstressed condition. Only a limited number of E3 ubiquitin ligases were found to function in degrading TFs under dehydration. This can be seen in knockout mutants of specific E3 ligases, which allowed the expression of specific TFs and influenced the stress tolerance of Arabidopsis plants. When the cognate E3 ligase genes *DRIP1/DRIP2* (Qin et al., 2008), *AIP2* (Zhang et al., 2005), and *RGLG1/RGLG2* (this study) were knocked out, the respective TFs, DREB2A, ABI3, and AtERF53, could be detected in cells and conferred dehydration tolerance. This also occurs in other stressful conditions; when *HOS1* (a RING E3 ligase) was knocked out, the overexpression of *ICE1* (an MYC-like basic helix-loop-helix TF) conferred freezing tolerance to plants (Dong et al., 2006).

In this research, a yeast two-hybrid analysis and BiFC assay confirmed the interaction between AtERF53 and RGLG2. As reported by Yin et al. (2007), the functionally redundant ubiquitin ligases, RGLG1 and RGLG2, are expressed at the plasma membrane but are also present at the membrane of dynamically formed cytoplasm strands (Yin et al., 2007). Since AtERF53-GFP was observed in nuclei, the RGLG2 protein may require posttranslational modification or the presence of carrier proteins for nuclear import and protein-protein interactions under stress conditions. We have also performed subcellular localization analysis of RGLG2 to see whether RGLG2 would enter the nucleus in PEG-transfected protoplasts. As we have observed, RGLG2 was localized in the nuclei and was also present as an accumulated form at the plasma membrane (Fig. 4A). The localization difference between permanent transgenic plants (Yin et al., 2007) and transiently expressed protoplasts might result from the osmotic stress (PEG treatment) given to protoplasts. According to our observations, RGLG2 actually entered the nucleus under stress conditions (Fig. 4B), which suggests that RGLG2 might translocate to the nucleus by some unknown mechanisms. The RING domain of the E3 ligase was found to be essential for E3 ligase activity, and its C-terminal conserved region is responsible for protein interactions (Qin et al., 2008). Our β-galactosidase activity

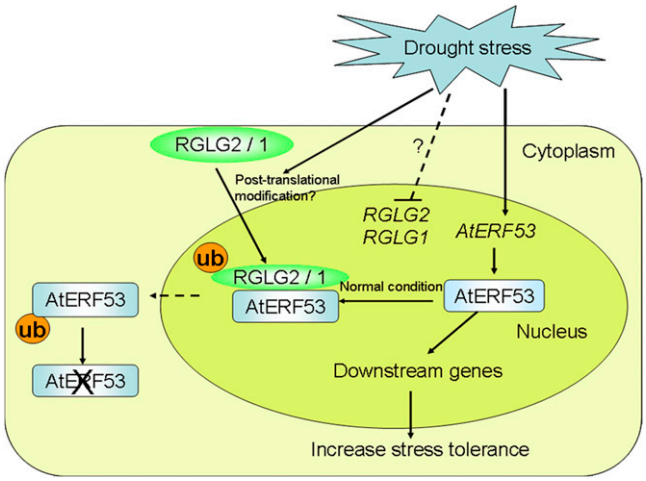

Figure 8. A model of RGLG1 and RGLG2 regulating drought stress signaling by mediating AtERF53 degradation. During drought stress, *AtERF53* is induced to activate downstream gene expression. It is possible that *RGLG1* and *RGLG2* are down-regulated or that the ubiquitination and proteolysis processes are blocked in the early hours of drought stress stimulus. Under normal conditions, AtERF53 is recognized and ubiquitinated by RGLG2 and RGLG1 via an unknown posttranslational modification and then subjected to 26S proteasome proteolysis. The AtERF53-mediated drought stress response is thereby prevented.

assay results also supported the truncated RGLG2 (copine region) being more interactive with AtERF53, suggesting that posttranslational modification or domain masking might be necessary for AtERF53-RGLG2 interactions.

RGLG2 and *RGLG1* are generally expressed in the whole plant, with stronger expression in the vasculature (Yin et al., 2007). One notable thing is that *AtERF53* was also highly expressed in the vasculature, as we found in this study. This evidence further clarifies that the regulation of AtERF53 by RGLG2/RGLG1 is possible because of their spatial patterns. The spatial expression patterns observed in *promoter*:*GUS* transgenic plants were similar to many TFs, such as AtMYB44, MYBC1, ANAC012, and HIPP26, which are also highly induced by many abiotic stresses (Ko et al., 2007; Jung et al., 2008; Barth et al., 2009; Zhai et al., 2010). The root system is responsible for water absorbance and transportation and is the first organ to detect a water deficiency in the soil. High expression levels of GUS activity observed in roots and vascular bundles suggest that AtERF53 may function in the rapid drought stress response and long-distance signal transduction to mount a systemic defense in Arabidopsis plants. Interestingly, the expression patterns that were identified in leaves were not observed in guard cells, suggesting that AtERF53 does not function in stomatal closure for water conservation.

RGLG2 is categorized as being in the RING-HCa subgroup, as is COP1, which represses photomorphogenesis by targeting activators of light-responsive genes for degradation (Hardtke et al., 2000). As far as we know, only limited reports support RING domain-containing proteins functioning as E3 ligases. RGLG2 and RGLG1 both function in proteasomal degradation (this study) and are also associated with nonproteolytic signaling (Yin et al., 2007). This property of E3 ligases probably is not uncommon, because AtCHIP (a CHIP-like protein in Arabidopsis) is another E3 ligase that functions in proteasomal degradation (Shen et al., 2007) and is also associated with nonproteolytic signaling (Luo et al., 2006). In addition, RGLG proteins function in aspects of epidermal development; the *rglg1rglg2* mutant showed constitutive formation of branched root hairs independent of the iron supply, indicating the involvement of polyubiquitination in the altered differentiation of rhizodermal cells (Li and Schmidt, 2010). It seems that some ubiquitin domain E3 ligase genes are constitutively expressed, such as *RGLG2/RGLG1* and *DRIP1/DRIP2* genes, while others are induced in response to stress. It was generalized that these E3 ligases may function as regulators during various abiotic stress responses (Cho et al., 2008).

In vitro ubiquitination assays in the presence of ubiquitin, rabbit E1, and human UBCH5c (E2) showed that RGLG2 displays E3 ligase activity and mediates the ubiquitination of AtERF53. RGLG2 was reported to regulate apical dominance in Arabidopsis by forming a ubiquitin Lys-63 chain, whereas the formation of Lys-48-linked chains targets substrates that are recognized and degraded by the proteasome (Yin et al., 2007). RGLG2 is specific for ubiquitin Lys-63 linkages in the presence of UBC35 and MMZ2 (Arabidopsis homologs for Ubc13 and Mms2, respectively, which form regulatory-type ubiquitin Lys-63 chains in animals and yeast). Predominant ubiquitin signals for protein degradation appear to be the Lys-48-linked ubiquitin chain; however, ubiquitin chains of other linkage types were also reported (Johnson et al., 1995). Future studies are necessary to confirm the ability of RGLG2 to form Lys-48 chains and in vivo ubiquitination of AtERF53.

The finding that RGLG2/RGLG1, the specific E3 ligase, targets the AtERF53 protein for degradation explains why we could not obtain *AtERF53* overexpressor at the beginning. The *rglg1rglg2* double mutants displayed significant drought tolerance when compared with wild-type plants. We proved that the AtERF53 protein is more stable and is the target TF conferring drought tolerance in double mutants. P5CS1 is a key enzyme involved in the Pro synthesis pathway. The accumulation of Pro in plant cells can protect the cells from osmotic stress (Hong et al., 2000). The expression level of *P5CS1* in *35S*:*AtERF53-GFP*/*rglg1rglg2* was greater than that in wild-type plants, *rglg1rglg2* double mutants, and *35S*:*AtERF53-GFP*/Col-0, which might suggest that AtERF53 confers drought tolerance by way of the accumulation of a second metabolite (like Pro). The *COR15B* expression level was also examined as a drought-inducible marker gene, and *COR15B* might also be a downstream gene of AtERF53. Moreover, *35S*:*AtERF53-GFP/rglg1rglg2* transgenic plants exhibited higher drought tolerance than *rglg1rglg2* double mutants. This result further proved that AtERF53 is a positive regulator of drought tolerance.

In conclusion, we found that RGLG2, functioning as a RING domain E3 ligase, interacts with a drought-inducible TF, AtERF53. *AtERF53* induced during dehydration indeed plays a positive role in plant drought signaling and is recognized and ubiquitinated for 26S proteasome proteolysis under nonstressed conditions. RGLG2 mediates the ubiquitination and thus negatively regulates drought stress signaling. The degradation process might be inhibited temporarily once stress signaling occurs; consequently, plant cells may acquire efficient AtERF53 to activate stress-responsive gene expression (Fig. 8).

MATERIALS AND METHODS

Plant Materials and Transgenic Plant Construction

Throughout this study, *AtERF53* (*At2g20880*) *promoter*:*GUS*, *35S*:*AtERF53*, and *35S*:*AtERF53-GFP-His* transgenic lines were in the Col-0 ecotype of Arabidopsis (*Arabidopsis thaliana*). The promoter of *AtERF53* was amplified from Col-0 by the primer pair 5′-AAGTTTAATTGGAATAGCAAG-3′ and 5′-GTGGTTATGAAATATTTTCCCCAC-3′, using a high-fidelity PCR method, and then was inserted into pKGWFS7 to generate the *AtERF53 promoter*:*GUS* construct. The *AtERF53* coding sequence was amplified by the primer pair 5′-ATGGCTACTGCTAAGAACAAGGG-3′ and 5′-AATTGTAT-

CAGAAGAAGAGT-3′ and was inserted into pB2GW7 and pEarleyGate103 to generate *35S:AtERF53* and *35S:AtERF53-GFP-His* transgenic plants, respectively. The constructed plasmids were introduced into *Agrobacterium tumefaciens* GV3101 cells. Seeds were sown in a 2:2:1 mixture of vermiculite, perlite, and peat moss, incubated in the dark for 2 to 4 d at 4°C, and transferred to a growth chamber for germination. The *35S:AtERF53*, *35S:AtERF53-GFP-His*, and *35S:AtERF53-GFP-His/rglg1rglg2* transgenic plants were screened with Basta after 2 weeks of incubation. For the *AtERF53 promoter:GUS* transgenic lines screened on MS medium (pH 5.6) containing 1% Suc, 0.8% phytoagar, and 50 μL L^{-1} kanamycin, seeds were surface sterilized with 75% ethanol and 7 μL of 30% (v/v) Tween 20 (for 1 mL of ethanol) for 15 min and for another 15 min with 95% ethanol. After removing the 95% ethanol, autoclaved distilled water was added before growing on MS medium. Seedlings were grown under a 16/8-h light/dark photoperiod at 22°C at a light intensity of 100 to 150 μmol m^{-2} s^{-1}. The *rglg1* and *rglg2* single mutant and *rglg1rglg2* double mutant Arabidopsis plants were obtained from Prof. Andreas Bachmair (Yin et al., 2007). The *35S:AtERF53-GFP-His* construct was introduced into the *rglg1rglg2* double mutant to generate *35S:AtERF53-GFP-His/rglg1rglg2* transgenic Arabidopsis plants.

For drought treatment, Arabidopsis plants were germinated and grown on a sterilized mesh overlaid on MS agar for 2 weeks. The mesh was removed from the agar and placed on a new petri dish for dehydration. Total RNA or protein was isolated from dehydrated leaves at different time points.

For chemical treatments, solutions of 100 μM (±)-ABA (Sigma product no. A-1049), 100 mM jasmonic acid, 50 mM ACC, 10 μM hydrogen peroxide, 300 mM NaCl, and 500 mM mannitol were applied to the surface of solid MS agar medium in which 2-week-old seedlings were growing. Petri dishes were then sealed with Parafilm.

RNA Preparation, Real-Time PCR, and RNA Gel-Blot Analysis

Total RNA was isolated with REzol C&T (PROtech Technologies; http://www.bio-protech.com.tw/), and 10 μg of total RNA was separated on a 1.2% formaldehyde agarose gel, blotted onto a positively charged nylon membrane (Roche; http://www.roche.com/), and hybridized at 65°C with full-length *AtERF53* coding sequence fragments labeled with digoxigenin-11-dUTP by PCR. The primer sequences were 5′-ATGGCTACTGCTAAGAACAAGG-3′ and 5′-AATTGTATCAGAAGAAGAGTTT-3′. The membrane was washed twice at 65°C for 10 min in 2× sodium chloride/sodium phosphate/EDTA buffer supplemented with 0.1% (w/v) SDS. Hybridization signals were detected by the chemiluminescent reaction with disodium 3-(4-methoxyspiro{1,2,-dioxetane-3,2′-(5′-chloro)tricyclo[3.3.1.1]decan}-4-yl)phenyl phosphate (Roche).

Histochemical GUS Staining and GFP Fluorescence Observation

The GUS expression patterns of tissues from various organs either from soil-grown transgenic plants or seedlings grown on half-strength MS were analyzed. The GUS staining solution contained 100 mM sodium phosphate buffer (pH 7.0), 0.5 mg mL^{-1} 5-bromo-4-chloro-3-indolyl β-D-glucuronic acid (Duchefa; http://www.duchefa.com/), 0.1% Triton, and 0.5 mM each of potassium ferricyanide/ferrocyanide. Samples were vacuum infiltrated for 15 to 30 min and incubated at 37°C for 16 to 24 h. Plant tissues were then fixed in 4% formaldehyde, 50% ethanol, and 5% acetic acid, dehydrated in an ethanol series, and infiltrated with Histo-Clear (International Diagnostics) followed by Paraffin. Observation was conducted with a light microscope (MZ16F; Leica), and an RS Photometrics CoolSNAP camera (DFC490; Leica) was used to take the digital images, with the corresponding IM50 software. GFP fluorescence was observed with a laser scanning confocal microscope (TCS SP5 AOBS; Leica).

Yeast Two-Hybrid Screening and Interaction Assay

An Arabidopsis cDNA library was prepared in the pGADT7 vector (MatchMaker GAL4 two-hybrid system 3; Clontech; http://www.clontech.com/) using mRNA isolated from 3-week-old plants. Yeast transformation was performed according to the supplier's instructions (Clontech). β-Galactosidase activity was determined in AH109 yeast report cells as described in the Yeast Protocols Handbook (Clontech).

BiFC Assays

RGLG2 and AtERF53 full-length sequences were cloned into the cCFP and nVenus vectors, respectively. The two vectors were kindly provided by S.B. Gelvin (Department of Biological Sciences, Purdue University), with *Sal*I-*Bam*HI and *Hin*dIII-*Eco*RI sites, respectively, after the 35S promoter sequence. Transient expression in Arabidopsis protoplasts was analyzed following Jen Shen's laboratory protocol (Yoo et al., 2007). YFP fluorescence was observed with a laser scanning confocal microscope (Leica TCS SP5).

Fusion Protein Preparation

Recombinant GST fusion proteins were prepared as described in the GE Protocol Handbook (www.gelifesciences.com/protein-purification). Fragments encoding AtERF53 were PCR amplified from drought-treated cDNA with the following primers: 5′-CTCGGATCC**ATG**GCTACTGCTAAGAA-3′ (the *Bam*HI site is underlined and the ATG is boldface) and 5′-ACAGAATTCCTAAATTGTATCAGAAGAAGA-3′ (the *Eco*RI site is underlined). The PCR fragments were ligated into pGEM-T Easy (Promega; http://www.promega.com/) for DNA sequencing by Tri-I Biotech using an ABI 3730 sequencer (Applied Biosystems). The recombinant plasmids were cut with *Bam*HI and *Eco*RI and ligated into pGEX-6p-1 (Amersham Pharmacia Biotech). The resulting plasmids were transformed into *Escherichia coli* DH5α and then induced by 1 mM isopropylthio-β-galactoside for expression in host BL21 (DE3) cells. Recombinant fusion proteins were affinity purified from bacterial lysates using glutathione-Sepharose (Amersham-Pharmacia) according to the manufacturer's procedures and then stored at −30°C.

In Vitro Ubiquitination Assays and Protein Gel-Blot Analysis

The ubiquitination assays were generally performed as described by Xie et al. (2002). Approximately 500 ng of the RGLG2-GST fusion protein was mixed with 100 ng of rabbit E1 (Enzo Life Sciences; http://www.enzolifesciences.com/), 200 ng of human E2 UBCH5C (Enzo Life Sciences), and 5 mg of ubiquitin (Enzo Life Sciences)/ubiquitin (Sigma-Aldrich; http://www.sigmaaldrich.com/). The reactions were made in buffer containing 50 mM Tris-HCl (pH 7.4), 5 mM $MgCl_2$, 2 mM ATP, 2 mM dithiothreitol, 10 mM phosphocreatine, and 1 unit of creatine kinase (Sigma-Aldrich). After incubation at 30°C for 2 h, the reaction was stopped with 2× SDS sampling buffer by boiling at 100°C for 5 min. Ten microliters of each reaction was analyzed by SDS-PAGE and immunoblot analysis using a corresponding antibody. To confirm that RGLG2 mediates At2g20880 ubiquitination, the At2g20880-His-Trx fusion protein was affinity purified and 200 ng of the purified protein was incubated together with the ubiquitination mixture for 2 h. The mixture was then subjected to 6% SDS-PAGE and immunoblot analysis. For the anti-GFP immunoblot analysis, the nuclear fraction was prepared according to the methods of Busk and Pages (1997) with minor modifications. Eighteen micrograms of protein was loaded and blotted for immunodetection with a monoclonal anti-GFP primary antibody (Santa Cruz Biotechnology; http://www.scbt.com/).

Stress Tolerance Tests

For the drought tolerance test, plants were initially grown on soil under a normal watering regime for 3 weeks. Watering was then halted and observations were made after a further 14 to 16 d without water. When wild-type plants exhibited lethal effects of dehydration, watering was resumed, and the plants were allowed to grow for a subsequent 5 d. The survival rate was scored.

Supplemental Data

The following materials are available in the online version of this article.

Supplemental Figure S1. RNA gel-blot analyses of *AtERF53* expression by different hormones.

Supplemental Figure S2. In vitro pull-down assays of Trx-AtERF53 protein with GST-RGLG2 fusion protein.

Supplemental Figure S3. The interaction and E3 ligase activities of RGLG1 with AtERF53.

Supplemental Figure S4. Expression profiles of *RGLG1* and *RGLG2* on the eFP browser.

Supplemental Figure S5. Drought tolerance test of wild-type plants, *rglg1rglg2*, and *35S:RGLG2/rglg1rglg2* (RG2OE).

Supplemental Figure S6. Pro content in wild type, *rglg1rglg2*, and *35S:AtERF53-GFP/rglg1rglg2*.

Supplemental Table S1. Positive clones from yeast two-hybrid screening.

ACKNOWLEDGMENTS

We thank Prof. Andreas Bachmair for providing *rglg1rglg2*, *rglg1*, and *rglg2* mutants and helpful comments on the manuscript. We are grateful to the staffs of TC5 Bio-Image Tools, Technology Commons, College of Life Science, National Taiwan University, for help with the confocal laser scanning microscopy.

Received October 20, 2011; accepted November 17, 2011; published November 17, 2011.

LITERATURE CITED

Barth O, Vogt S, Uhlemann R, Zschiesche W, Humbeck K (2009) Stress induced and nuclear localized HIPP26 from Arabidopsis thaliana interacts via its heavy metal associated domain with the drought stress related zinc finger transcription factor ATHB29. Plant Mol Biol **69:** 213–226

Busk PK, Pages M (1997) Microextraction of nuclear proteins from single maize embryo. Plant Mol Biol Rep **15:** 371–376

Cho SK, Ryu MY, Song C, Kwak JM, Kim WT (2008) *Arabidopsis* PUB22 and PUB23 are homologous U-box E3 ubiquitin ligases that play combinatory roles in response to drought stress. Plant Cell **20:** 1899–1914

Dong CH, Agarwal M, Zhang Y, Xie Q, Zhu JK (2006) The negative regulator of plant cold responses, HOS1, is a RING E3 ligase that mediates the ubiquitination and degradation of ICE1. Proc Natl Acad Sci USA **103:** 8281–8286

Glickman MH, Ciechanover A (2002) The ubiquitin-proteasome proteolytic pathway: destruction for the sake of construction. Physiol Rev **82:** 373–428

Gong W, He K, Covington M, Dinesh-Kumar SP, Snyder M, Harmer SL, Zhu Y-X, Deng XW (2008) The development of protein microarrays and their applications in DNA-protein and protein-protein interaction analyses of Arabidopsis transcription factors. Mol Plant **1:** 27–41

Haake V, Cook D, Riechmann JL, Pineda O, Thomashow MF, Zhang JZ (2002) Transcription factor CBF4 is a regulator of drought adaptation in Arabidopsis. Plant Physiol **130:** 639–648

Hardtke CS, Gohda K, Osterlund MT, Oyama T, Okada K, Deng XW (2000) HY5 stability and activity in Arabidopsis is regulated by phosphorylation in its COP1 binding domain. EMBO J **19:** 4997–5006

Hong Z, Lakkineni K, Zhang Z, Verma DPS (2000) Removal of feedback inhibition of delta(1)-pyrroline-5-carboxylate synthetase results in increased proline accumulation and protection of plants from osmotic stress. Plant Physiol **122:** 1129–1136

Johnson ES, Ma PC, Ota IM, Varshavsky A (1995) A proteolytic pathway that recognizes ubiquitin as a degradation signal. J Biol Chem **270:** 17442–17456

Jung C, Seo JS, Han SW, Koo YJ, Kim CH, Song SI, Nahm BH, Choi YD, Cheong JJ (2008) Overexpression of AtMYB44 enhances stomatal closure to confer abiotic stress tolerance in transgenic Arabidopsis. Plant Physiol **146:** 623–635

Knight H, Zarka DG, Okamoto H, Thomashow MF, Knight MR (2004) Abscisic acid induces CBF gene transcription and subsequent induction of cold-regulated genes via the CRT promoter element. Plant Physiol **135:** 1710–1717

Ko JH, Yang SH, Park AH, Lerouxel O, Han KH (2007) ANAC012, a member of the plant-specific NAC transcription factor family, negatively regulates xylary fiber development in Arabidopsis thaliana. Plant J **50:** 1035–1048

Kraft E, Stone SL, Ma L, Su N, Gao Y, Lau OS, Deng XW, Callis J (2005) Genome analysis and functional characterization of the E2 and RING-type E3 ligase ubiquitination enzymes of Arabidopsis. Plant Physiol **139:** 1597–1611

Lee LY, Fang MJ, Kuang LY, Gelvin SB (2008) Vectors for multi-color bimolecular fluorescence complementation to investigate protein-protein interactions in living plant cells. Plant Methods **4:** 24–34

Li W, Schmidt W (2010) A lysine-63-linked ubiquitin chain-forming conjugase, UBC13, promotes the developmental responses to iron deficiency in Arabidopsis roots. Plant J **62:** 330–343

Lin RC, Park HJ, Wang HY (2008) Role of Arabidopsis RAP2.4 in regulating light- and ethylene-mediated developmental processes and drought stress tolerance. Mol Plant **1:** 42–57

Liu Q, Kasuga M, Sakuma Y, Abe H, Miura S, Yamaguchi-Shinozaki K, Shinozaki K (1998) Two transcription factors, DREB1 and DREB2, with an EREBP/AP2 DNA binding domain separate two cellular signal transduction pathways in drought- and low-temperature-responsive gene expression, respectively, in *Arabidopsis*. Plant Cell **10:** 1391–1406

Luo J, Shen G, Yan J, He C, Zhang H (2006) AtCHIP functions as an E3 ubiquitin ligase of protein phosphatase 2A subunits and alters plant response to abscisic acid treatment. Plant J **46:** 649–657

Nakano T, Suzuki K, Fujimura T, Shinshi H (2006) Genome-wide analysis of the ERF gene family in Arabidopsis and rice. Plant Physiol **140:** 411–432

Ohme-Takagi M, Shinshi H (1995) Ethylene-inducible DNA binding proteins that interact with an ethylene-responsive element. Plant Cell **7:** 173–182

Pickart CM (2001) Mechanisms underlying ubiquitination. Annu Rev Biochem **70:** 503–533

Pickart CM, Eddins MJ (2004) Ubiquitin: structures, functions, mechanisms. Biochim Biophys Acta **1695:** 55–72

Qin F, Sakuma Y, Tran LS, Maruyama K, Kidokoro S, Fujita Y, Fujita M, Umezawa T, Sawano Y, Miyazono K, et al (2008) *Arabidopsis* DREB2A-interacting proteins function as RING E3 ligases and negatively regulate plant drought stress-responsive gene expression. Plant Cell **20:** 1693–1707

Sakuma Y, Liu Q, Dubouzet JG, Abe H, Shinozaki K, Yamaguchi-Shinozaki K (2002) DNA-binding specificity of the ERF/AP2 domain of Arabidopsis DREBs, transcription factors involved in dehydration- and cold-inducible gene expression. Biochem Biophys Res Commun **290:** 998–1009

Sakuma Y, Maruyama K, Osakabe Y, Qin F, Seki M, Shinozaki K, Yamaguchi-Shinozaki K (2006) Functional analysis of an *Arabidopsis* transcription factor, DREB2A, involved in drought-responsive gene expression. Plant Cell **18:** 1292–1309

Seki M, Narusaka M, Ishida J, Nanjo T, Fujita M, Oono Y, Kamiya A, Nakajima M, Enju A, Sakurai T, et al (2002) Monitoring the expression profiles of 7000 Arabidopsis genes under drought, cold and high-salinity stresses using a full-length cDNA microarray. Plant J **31:** 279–292

Shen G, Adam Z, Zhang H (2007) The E3 ligase AtCHIP ubiquitylates FtsH1, a component of the chloroplast FtsH protease, and affects protein degradation in chloroplasts. Plant J **52:** 309–321

Shinozaki K, Yamaguchi-Shinozaki K (2007) Gene networks involved in drought stress response and tolerance. J Exp Bot **58:** 221–227

Smalle J, Vierstra RD (2004) The ubiquitin 26S proteasome proteolytic pathway. Annu Rev Plant Biol **55:** 555–590

Stone SL, Hauksdóttir H, Troy A, Herschleb J, Kraft E, Callis J (2005) Functional analysis of the RING-type ubiquitin ligase family of Arabidopsis. Plant Physiol **137:** 13–30

Thomashow MF (1999) Plant cold acclimation: freezing tolerance genes and regulatory mechanisms. Annu Rev Plant Physiol Plant Mol Biol **50:** 571–599

Yamaguchi-Shinozaki K, Shinozaki K (1994) A novel cis-acting element in an *Arabidopsis* gene is involved in responsiveness to drought, low-temperature, or high-salt stress. Plant Cell **6:** 251–264

Yee D, Goring DR (2009) The diversity of plant U-box E3 ubiquitin ligases: from upstream activators to downstream target substrates. J Exp Bot **60:** 1109–1121

Yin XJ, Volk S, Ljung K, Mehlmer N, Dolezal K, Ditengou F, Hanano S, Davis SJ, Schmelzer E, Sandberg G, et al (2007) Ubiquitin lysine 63

chain forming ligases regulate apical dominance in *Arabidopsis*. Plant Cell **19:** 1898–1911

Yoo SD, Cho YH, Sheen J (2007) Arabidopsis mesophyll protoplasts: a versatile cell system for transient gene expression analysis. Nat Protoc **2:** 1565–1572

Vierstra RD (2009) The ubiquitin-26S proteasome system at the nexus of plant biology. Nat Rev Mol Cell Biol **10:** 385–397

Xie Q, Guo HS, Dallman G, Fang S, Weissman AM, Chua NH (2002) SINAT5 promotes ubiquitin-related degradation of NAC1 to attenuate auxin signals. Nature **419:** 167–170

Zhai H, Bai X, Zhu Y, Li Y, Cai H, Ji W, Ji Z, Liu X, Liu X, Li J (2010) A single-repeat R3-MYB transcription factor MYBC1 negatively regulates freezing tolerance in Arabidopsis. Biochem Biophys Res Commun **394:** 1018–1023

Zhang X, Garreton V, Chua NH (2005) The AIP2 E3 ligase acts as a novel negative regulator of ABA signaling by promoting ABI3 degradation. Genes Dev **19:** 1532–1543